ARTICLES

# The neural basis of *Drosophila* gravity-sensing and hearing

Azusa Kamikouchi[1,2,3]*, Hidehiko K. Inagaki[2]*†, Thomas Effertz[1,4], Oliver Hendrich[1,4], André Fiala[4,5], Martin C. Göpfert[1,4] & Kei Ito[2]

**The neural substrates that the fruitfly *Drosophila* uses to sense smell, taste and light share marked structural and functional similarities with ours, providing attractive models to dissect sensory stimulus processing. Here we focus on two of the remaining and less understood prime sensory modalities: graviception and hearing. We show that the fly has implemented both sensory modalities into a single system, Johnston's organ, which houses specialized clusters of mechanosensory neurons, each of which monitors specific movements of the antenna. Gravity- and sound-sensitive neurons differ in their response characteristics, and only the latter express the candidate mechanotransducer channel NompC. The two neural subsets also differ in their central projections, feeding into neural pathways that are reminiscent of the vestibular and auditory pathways in our brain. By establishing the *Drosophila* counterparts of these sensory systems, our findings provide the basis for a systematic functional and molecular dissection of how different mechanosensory stimuli are detected and processed.**

The fruitfly *Drosophila melanogaster* responds behaviourally to gravity and sound. When tapped down in a vial, the flies tend to walk up against the Earth's gravitational field, a directed behaviour that is known as negative gravitaxis or anti-geotaxis[1–3]. When exposed to male courtship songs, females reduce locomotion whereas males start chasing each other, forming so-called courtship chains[4,5]. Both *Drosophila* gravitaxis and sound communication have long been prime paradigms for the genetic dissection of behaviour[1–5], but the underlying sensory mechanisms are poorly understood. The human ability to sense gravity and sound relies on specialized vestibular and auditory organs in our inner ear[6,7]. In the fly, the ability to hear has been ascribed to the antenna[5,8–14]: the club-shaped third segment and the distal arista (formed by the fourth to sixth segments) of the antenna sympathetically vibrate in response to acoustic stimuli and, analogous to our eardrum, serve the reception of sound[12,14]. Vibrations of this antennal receiver are picked up by Johnston's organ (JO), a chordotonal stretch-receptor organ with ~480 primary sensory neurons in the second segment of the antenna (Fig. 1a). These JO neurons have also been surmised to have a role in gravity sensing[2,15]. The antennal receiver of the fly is predicted to deflect in response to gravitational forces (see Supplementary Information footnote 1), but physiological evidence exploring the role of JO neurons in gravity sensing has not been reported so far.

Here we examine the role of *Drosophila* JO neurons in gravity and sound detection. It has been shown that the JO neurons of the fly can be anatomically categorized into five subgroups, A–E, each of which targets a distinct area of the brain[13]. Whether this anatomical diversity is paralleled by function, however, has remained unclear[16]. We show that JO neuron subgroups are functionally specialized in that they preferentially respond to distinct types of antennal movement. We further show that this functional diversity reflects distinct behavioural requirements, with different JO neuron subgroups being needed for the response of flies to gravity and sound. These neural subgroups differ genetically and feed into distinct neural pathways in the brain. We have traced these newly identified sensory pathways and provide tools to dissect their function.

## Monitoring neural activities in JO

To assess directly neural activities in *Drosophila* JO caused by the antennal receiver movement, we have developed a live fly preparation that affords access to intracellular calcium signals in JO neurons through the cuticle of the antenna (Fig. 1a, b). An intact fly was mounted under a coverslip with the first and second antennal segments immobilized to prevent muscle-based antennal movements. The antennal receiver was kept freely moving, as was confirmed by laser Doppler vibrometric measurements of their mechanical fluctuations[17]. We mechanically actuated the antennal receiver by means of electrostatic force[17–19] (Fig. 1a and Supplementary Fig. 1a), and expressed a genetically encoded calcium sensor in JO neurons via the yeast-derived *GAL4/UAS* gene expression induction system, in which expression of reporter genes fused under *UAS* is activated specifically in the cells that express Gal4 (ref. 20). To distinguish mechanically evoked calcium signals from possible movement artefacts, we used the sensor cameleon 2.1 (Cam2.1)[21,22], which allows for ratiometric measurements of calcium-induced fluorescence resonance transfer (FRET) between enhanced cyan fluorescent protein (eCFP) and enhanced yellow fluorescent protein (eYFP).

When we expressed *cam2.1* in essentially all JO neurons by means of the *F-GAL4* driver[9] (JO-all > *cam2.1*), antennal movement evoked reciprocal changes in eCFP and eYFP fluorescence (Fig. 1c). These signals were largely reduced when *cam2.1* was expressed in homozygous *nanchung* (*nan*$^{36a}$) mutants[9], but not in heterozygous controls (Supplementary Fig. 1b). Like sound-evoked potentials in the antennal nerve of flies[9], mechanically evoked calcium signals in JO neuron somata thus depend on the transient receptor potential vanilloid (TRPV) channel Nanchung, providing additional evidence for the

[1]Sensory Systems Laboratory, Institute of Zoology, University of Cologne, 50923 Cologne, Germany. [2]Institute of Molecular and Cellular Biosciences, University of Tokyo, Yayoi, Bunkyo-ku, 113-0032 Tokyo, Japan. [3]School of Life Sciences, Tokyo University of Pharmacy and Life Sciences, 1432-1, Horinouchi, Hachioji, 192-0392 Tokyo, Japan. [4]Johann-Friedrich-Blumenbach-Institute, University of Göttingen, 37073 Göttingen, Germany. [5]Theodor-Boveri-Institute, Department of Genetics and Neurobiology, Julius-Maximilians-University of Würzburg, Am Hubland, 97074 Würzburg, Germany. †Present address: Division of Biology 216-76, California Institute of Technology, Pasadena, California 91125, USA.
*These authors contributed equally to this work.

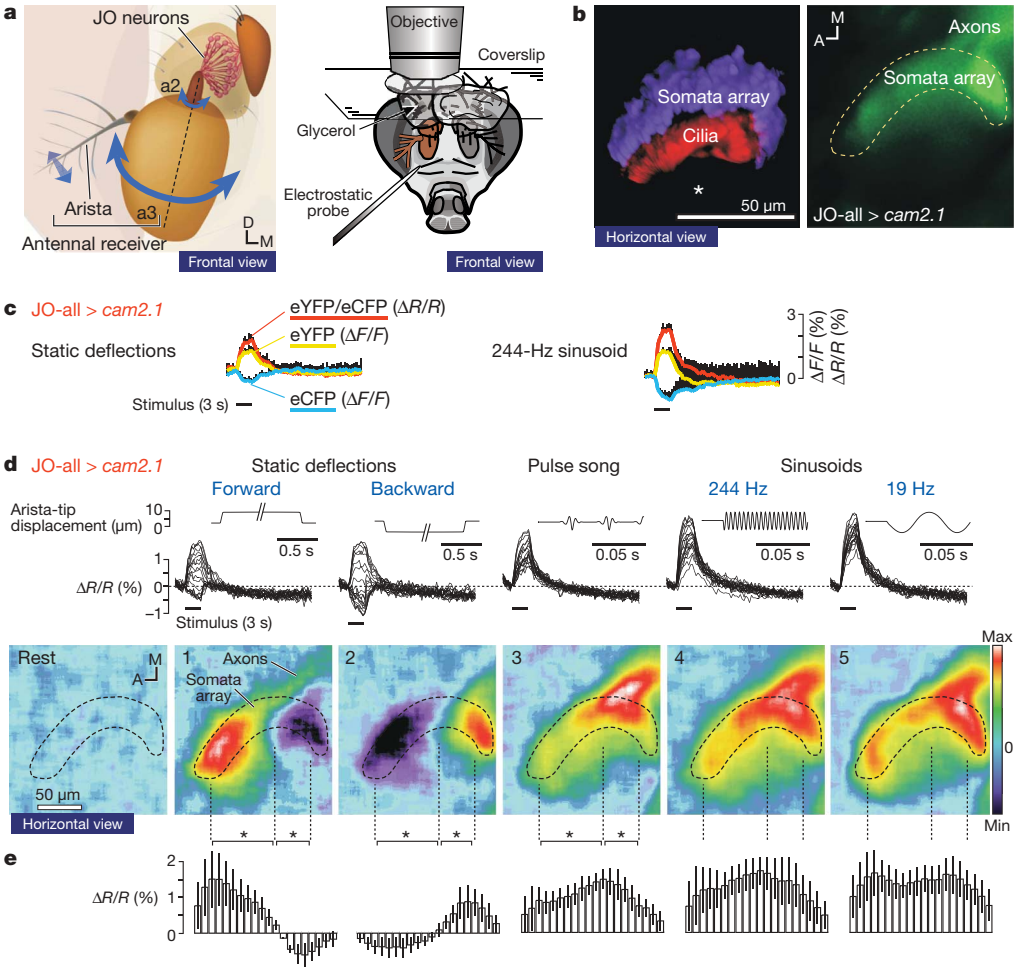


**Figure 1 | Mechanically evoked calcium signals in JO neurons.** **a**, Antennal anatomy and experimental setup. Left: in response to external forces, the third antennal segment (a3) and the arista twist back and forth (arrows) as a rigid body (antennal receiver), thereby activating JO neurons in the second antennal segment (a2). Right: stimulus forces were imposed on the arista by means of an electrostatic probe, eliciting calcium signals in JO neurons that were monitored with a fluorescence microscope. D, dorsal; M, medial. **b**, Horizontal views of JO. Left: three-dimensional confocal projection. Nuclei and cilia of JO neurons are labelled with anti-Elav antibody (blue) and phalloidin (red). Asterisk: attachment site between JO neurons and a3. Right: cam2.1 fluorescence in a JO-all > *cam2.1* fly as seen through the cuticle of a2. A, anterior. **c**, Time traces of JO calcium signals. Mechanical stimuli evoked reciprocal fluorescent changes ($\Delta F/F$) between eCFP (blue line) and eYFP (yellow line) by FRET. $\Delta R/R$ (%) is the change in eYFP/eCFP fluorescence ratio, where $R$ is the average eYFP/eCFP ratio before stimulus onset and $\Delta R$ is the deviation from $R$ (mean and s.d.; $n = 5$ repetitions). Black horizontal bars: stimulus (duration 3 s). **d**, Top: superimposed time traces of responses of JO neurons across the somata array. Insets: arista-tip displacement. Bottom: pseudocoloured ratio changes. $^*P < 0.05$. **e**, Amplitude distribution of ratio changes across the JO somata array (mean ± s.d.; $n = 5$ animals).

functional significance of the measured calcium signals. A small response to static deflection was observed in *nan* mutants (Supplementary Fig. 1b), consistent with the role of Nan in electrical signal propagation rather than transduction suggested in a previous report[23].

## Stimulus-specific neural activities in JO

Because the fly's antennal receiver is suspended by a hinge between the second and third segments, it vibrates back and forth in response to acoustic stimuli[12,14] and will deflect backwards and forwards if the fly walks up or down (see Supplementary Information footnotes 1 and 2). By measuring calcium signals in various areas of the JO neuron somata array, we found that deflecting and vibrating the antennal receiver evokes different neural activity patterns in JO (Fig. 1d, e and Supplementary Video 1). When the receiver was deflected statically with a constant force stimulus, opposing calcium signals were seen in the anterior and posterior regions: deflecting the receiver forwards evoked positive signals in the anterior region and negative signals in the posterior one; backward deflection evoked signals of inversed sign (Fig. 1d, e, panels 1 and 2). Broadly distributed signals that peaked in or near the centre region of the somata array, in contrast, were evoked by receiver vibrations induced by recorded courtship songs (pulse song, interpulse interval of ~35 ms or 29 Hz, dominant pulse frequency of ~200 Hz) or sinusoids at high (244 Hz) or low (19 Hz) frequencies (Fig. 1d, e, panels 3–5).

The opposing calcium responses against static deflections are likely to reflect the opposing arrangement of the JO neurons: the fly's JO neurons connect perpendicularly to the anterior and posterior sides of the antennal receiver[12,13,19]. As judged from the anatomy of this connection, deflecting the receiver forwards will stretch JO neurons in the anterior region and compress JO neurons in the posterior. Thus, JO neurons are activated (that is, depolarized) by stretch and deactivated (that is, hyperpolarized) by compression (see Supplementary Information footnote 3 for further discussion).

## Vibration- and deflection-sensitive JO neurons

Anatomically, the fly's JO neurons can be subdivided into five subgroups that target distinct zones of the antennal mechanosensory and motor centre (AMMC) in the brain[13] (Fig. 2b, Supplementary Fig. 2 and Supplementary Videos 2 and 3). Each JO neuron typically innervates only one zone of the AMMC, and neurons targeting the same zone

cluster together in JO[13]. To test whether these neural subgroups differ in function, we selectively expressed *cam2.1* using subgroup-specific *GAL4* drivers: JO-B strain for driving expression in JO neuron subgroup B (~100–150 neurons[13]), JO-AB[24] for subgroups A (~50–100 neurons[13]) and B, and JO-CE for subgroups C and E (together ~200 neurons[13]). (Subgroup D, with <30 neurons[13], was not investigated owing to the lack of specific driver lines.)

By using these lines, we found that JO neuron subgroups A and B (AB) and C and E (CE) respond preferentially to different stimulus types: whereas the former were activated maximally by receiver vibrations, the latter responded maximally to static receiver deflections (Fig. 2a, c). The deflection-evoked responses of subgroups CE persisted as long as the deflection was maintained, documenting tonic response characteristics of these neurons (Fig. 2d). The vibration-evoked responses of subgroups AB, in turn, were found to be frequency-dependent (Fig. 2e): when measured in combination, subgroup A and B neurons responded to receiver vibrations at broad frequency ranges between 19 Hz and 952 Hz. When measured alone, however, subgroup B displayed a clear preference for low-frequency vibrations, indicating that subgroup A mainly contributes to the high-frequency responses displayed by the combination of subgroups AB.

## JO neurons for gravity sensing

Functional imaging showed that JO neurons of subgroups CE respond preferentially to receiver deflections imposed by static stimuli such as gravitational force (Fig. 2 and Supplementary Fig. 3). To test whether these neurons are required for gravity sensing, we monitored the fly's negative gravitaxis behaviour in a countercurrent apparatus[25]. In this assay, flies are partitioned up into six tubes by giving them the choice five times to stay or to climb up the side of the tube (Fig. 3a and Supplementary Video 4). The partition coefficient Cf describing the final distribution ($0 < Cf < 1$) is large if the flies tend to climb up, and

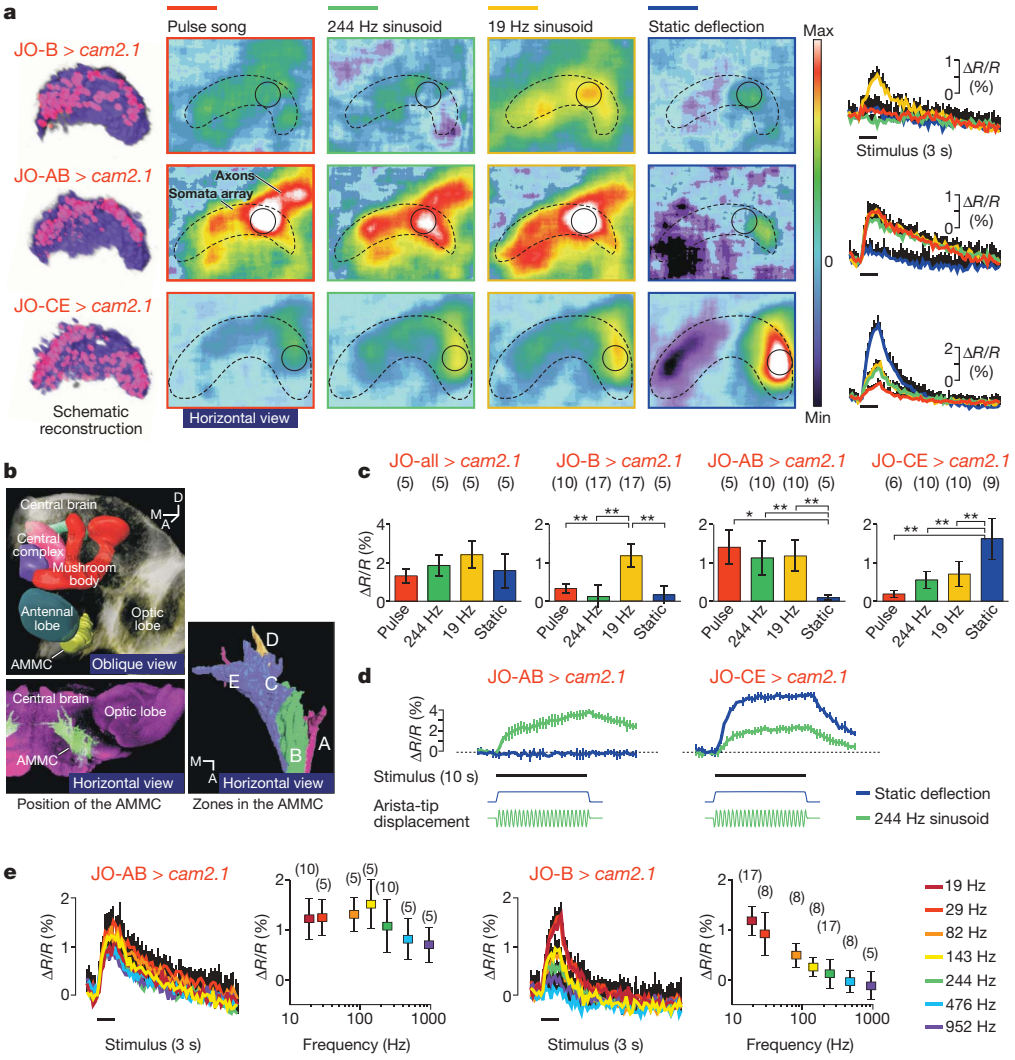


**Figure 2 | Responses of JO neuron subgroups. a**, Left: schematic horizontal view of the labelled neurons (magenta) and all somata (blue) of JO. Middle: representative pseudocolour images of ratio changes in JO neuron subgroups B, AB and CE evoked by four mechanical stimuli. Right: time traces obtained from the regions of the somata array of labelled neurons that, for given stimuli, showed the largest response (encircled by dashed lines in images, mean and s.d.; $n = 5$ repetitions). Note that absolute signal amplitudes may differ between fly strains owing to differences in labelled neuron numbers and expression levels. **b**, Architecture of the AMMC. Top left: location of the AMMC in the fly brain (schematic three-dimensional reconstruction of confocal serial sections). Bottom left: horizontal view of the brain at the level of the AMMC. Right: target zones of JO neuron subgroups in the AMMC. **c**, Average ratio change in the somata region that showed the largest response (mean ± s.d.; numbers in parentheses represent the number of animals). Subgroups AB respond preferentially to vibrations, and subgroups CE to static deflections. $^{*}P < 0.05$; $^{**}P < 0.01$. **d**, Superimposed time traces of the ratio changes to long stimuli (10 s, black horizontal bar) in subgroups AB (left) and CE (right) (mean ± s.d.; $n = 5$ repetitions). **e**, Time traces of ratio changes (mean ± s.d.; $n = 5$ repetitions, black horizontal bars indicate stimulus duration) and averaged ratio changes (mean ± s.d.; numbers in parentheses represent number of animals) in JO neuron subgroups AB (left two panels) and B (right two panels) measured at 19–952 Hz.

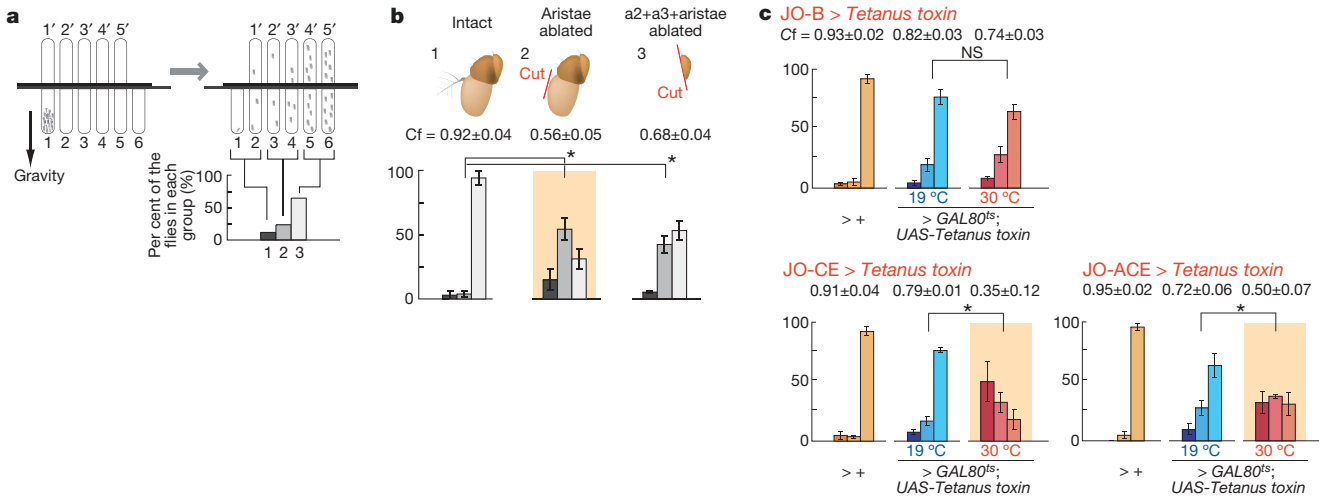


**Figure 3 | Requirement of JO neuron subgroups for gravity detection.** **a**, Negative gravitaxis assay. Numbers 1 to 6 and 1′ to 5′ represent the lower and upper tubes, respectively, from left to right. **b**, Wild-type flies with intact and ablated antennae. Cf, partition coefficient of the final distribution (mean ± s.e.m., >5 trials for each experimental group, see Supplementary Information footnotes 4 and 5); *$P < 0.05$, Student's *t*-test. **c**, Flies with genetically silenced JO neurons (mean ± s.e.m., >5 trials for each experimental group). *$P < 0.05$, Student's *t*-test. Cases with aberrant behaviour are highlighted (Cf < 2/3; see Supplementary Information footnote 5). Negative gravitaxis is eliminated by silencing subgroups CE and ACE, but not B. NS, not significant. The *x* and *y* axes for **b** and **c** are the same as in **a**.

small if they tend to stay (see Supplementary Information footnotes 4 and 5). As expected, wild-type flies displayed negative gravitaxis behaviour (Fig. 3b). This behaviour, but not phototaxis (Supplementary Fig. 4a), was abolished when the antennal aristae were ablated (Fig. 3b, panel 2). Removing also the third and second antennal segments, the latter of which houses JO, yielded slightly higher Cf values (Fig. 3b, panel 3, $P < 0.1$ between panels 2 and 3). Apparently, when JO is lost, other sense organs may partially take over gravity sensing, for example, receptors on the neck and legs that have been implicated in gravity sensing in other insect species[2,26].

To silence selectively subgroups of JO neurons, we conditionally expressed tetanus toxin[27] using subgroup-specific *GAL4* drivers and *tubulin-GAL80$^{ts}$*, a temperature-sensitive blocker of Gal4 expressed ubiquitously by the tubulin promoter[28,29]. Tetanus toxin expression was activated shortly before behavioural experiments by raising the rearing temperature from 19 °C to 30 °C. Expressing tetanus toxin by means of JO-all and JO-AB *GAL4* drivers caused general locomotion defects as indicated by aberrant phototaxis, probably due to Gal4 expression elsewhere in the body (Supplementary Fig. 4b). When tetanus toxin was expressed by means of the drivers JO-B, JO-CE and JO-ACE, however, phototaxis was normal (Supplementary Fig. 4c). Using these lines, we found that silencing subgroups CE and ACE, but not subgroup B, abolishes gravitaxis (Fig. 3c). Hence, consistent with the physiological data, the fly's gravitaxis behaviour requires the deflection-sensitive JO neurons of subgroups CE.

## Vibration-responsive neurons are required for hearing

To determine which JO neurons are required for hearing, we next exposed groups of males to synthesized pulse-song of increasing intensity. This made wild-type males chase other males to form courtship chains[4] (Fig. 4a and Supplementary Video 5). Consistent with earlier reports[4], we found that ablating the distal antennal segments abolishes this sound-evoked behaviour (Fig. 4b, c). We further found that this behaviour specifically requires JO neurons of subgroup B: whereas expressing tetanus toxin in subgroup B impaired the male's chaining behaviour, the behaviour remained unaffected when tetanus toxin was targeted to subgroups CE or ACE (Fig. 4d and Supplementary Fig. 4d).

Although physiological data indicate a role of subgroup-A JO neurons in sound detection (Fig. 2), silencing these neurons did not affect responses to courtship song (Fig. 4d). One possible explanation is that the JO-ACE driver used in the behavioural experiments labels a fraction of subgroup-A neurons[13]; not all subgroup-A neurons were therefore silenced by tetanus toxin. Additional hints on solving the apparent conundrum were obtained when we investigated how ablating specific subgroups affects sound-evoked compound action potentials (CAPs; the sum of action potentials recorded extracellularly) in the antennal nerve[18,19]. We induced selective apoptosis by expressing ricin toxin A[30] under Gal4 control using the *eyFLP/FRT* system[31], which drives expression of flippase (FLP) enzyme by the enhancer fragment of *eyeless* (*ey*) gene. FLP induces recombination, which leads to the removal of a stop between two *FRT* sites to restrict *ricin toxin* expression to *GAL4*-expressing cells in the eye and antenna (Supplementary Fig. 5a–d). We then sinusoidally vibrated the antennal receiver while simultaneously monitoring the arista's displacement and the CAPs in the nerve. The amplitude of the CAP increased sigmoidally for the antennal displacement range of ~25 nm–1 μm in wild-type flies as well as in the flies in which JO neuron subgroups B or BCE were ablated (Fig. 4e), independent of the frequency of stimulation (Supplementary Fig. 5e), but the range shifted up to ~100 nm–4 μm when also subgroup A was ablated (Fig. 4e and Supplementary Fig. 5f). Hence, subgroup A is probably required for the detection of nanometre-range receiver vibrations as imposed by attenuated pulse-songs and/or the faint sine-songs of courting males[5].

## NompC is expressed in sound-sensitive neurons

To gain first insights into the molecular mechanisms that account for the functional differences between deflection- and vibration-sensitive JO neurons, we analysed which JO neurons express the candidate mechanotransducer channel NompC (no mechanoreceptor potential C, also known as TRPN1)[23,32]. To identify *nompC*-expressing neurons, we expressed *GAL4* under the control of the *nompC* promoter (*nompC-GAL4*)[33]. In contrast to *F-GAL4*, which expresses Gal4 under the control of the *nanchung* promoter and labels almost all JO neurons, only some JO neurons were labelled by *nompC-GAL4* (Fig. 5a). Projection analysis revealed that *nompC-GAL4* labels JO neurons of subgroups AB but not CE (Fig. 5b and Supplementary Fig. 6b). Hence, whereas the TRPV channel Nanchung is expressed by almost all JO neurons, the TRPN channel NompC seems specific for sound-sensitive JO neurons. This differential expression presumably explains why disrupting NompC reduces, but does not abolish, mechanically evoked responses in the fly's antennal nerve[34], supporting NompC as a candidate mechanotransducer for hearing and indicating that gravity transduction is independent of NompC.

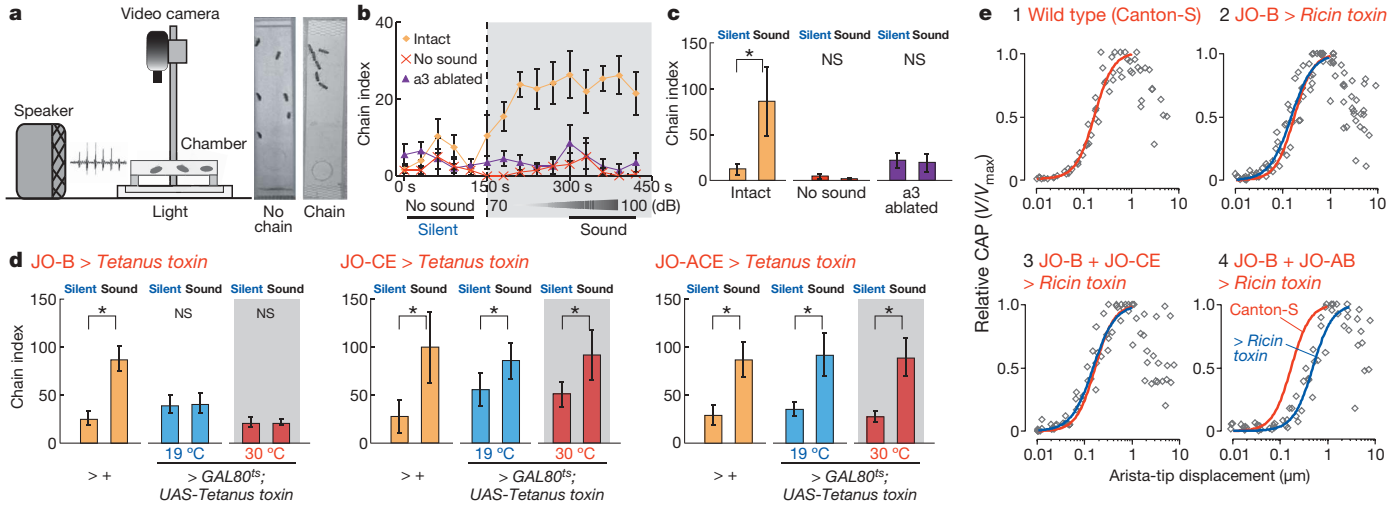


**Figure 4 | Requirement of JO neuron subgroups for hearing.** **a**, Courtship-song-detection assay. Representative images taken from videos of flies forming a courtship chain are shown. **b**, Time course of chain formation. Wild-type flies form chains only if the antenna is intact and in the presence of sound. **c**, Chain indices for flies in **b**. **d**, Chain indices for flies with genetically silenced JO neurons (mean ± s.e.m., >5 trials for each experimental group). Grey boxes: neurons silenced. Silencing subgroup B, but not subgroups CE and ACE, eliminates the formation of courtship chains. JO-B > *Tetanus toxin* flies fail to form chains even at 19 °C, probably due to leaky GAL80$^{ts}$ suppression. *$P < 0.05$; NS: $P > 0.05$, Mann–Whitney U-tests. **e**, Amplitude of sound-evoked CAPs in the antennal nerve as function of arista-tip displacement in ricin-toxin-expressing flies and controls. In panels 3 and 4, two *GAL4* driver lines were crossed to ablate larger cell populations. Blue, average fits for each genotypes; red, repeated in each panel, average fit for wild-type controls.

## Central circuits for gravity and sound

As judged from their central projections, gravity- and sound-sensitive JO neurons target distinct primary centres in the AMMC and feed into distinct brain circuits. To trace these circuits, we screened 3,939 *GAL4* enhancer trap lines[35] for higher-order neurons in the *Drosophila* brain that arborize in the AMMC. The target zones of subgroups A and B in the AMMC, which form the primary auditory centres, are both characterized by a close association with the inferior part of the ventrolateral protocerebrum (VLP), which is also directly supplied by a subset of subgroup-A neurons[13] and can be regarded as the secondary auditory centre: various interneurons were identified that arborize in both the VLP and the target zones of subgroups AB in the AMMC (Fig. 6a and Supplementary Fig. 6a, see also Supplementary Information footnote 6). These zones are also characterized by extensive commissural connections, with interneurons connecting the contralateral zones by means of commissures above and below the oesophagus (Fig. 6a and Supplementary Fig. 7). Also the giant fibre neuron (GFN), a large descending neuron that controls jump escape behaviour[36,37], arborizes in zone A and in the inferior VLP (Fig. 6a, see also Supplementary Information footnote 7). The GFNs of both sides are connected by means of the giant commissural interneurons[37], a feature not observed in the other descending neurons described below. All higher-order neurons we identified arborized only in the target zone of either subgroup A or B, pointing to a parallel organization of the auditory pathway that might explain why silencing only one subgroup of vibration-sensitive neurons suffices to abolish the flies' sound-evoked behaviour.

Aside from a few JO neurons of subgroups CE that directly cross the midline[13], we did not find commissural connections between the target zones of subgroups CE (Supplementary Fig. 7). No connections

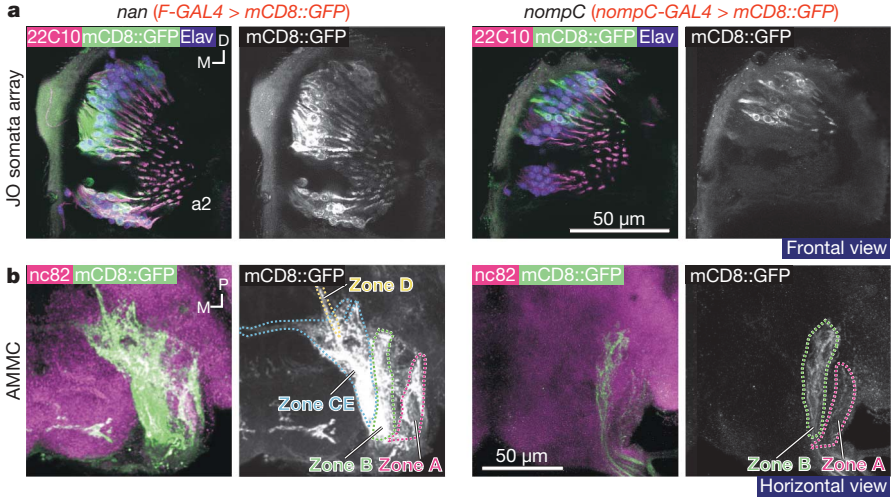


**Figure 5 | Expression of *nan* and *nompC*.** **a**, Distribution of *nan*- and *nompC*-expressing neurons in JO (confocal projections). JO neurons are visualized by 22C10 antibody (magenta) and a pan-neural marker, anti-Elav antibody (blue). Left: *F-GAL4*, in which *GAL4* is fused to the *nan* promoter, drives the expression of mCD8::GFP reporter proteins (green) in virtually all JO neurons. Right: only a subset of JO neurons is labelled if *GAL4* is fused to the promoter of *nompC*. **b**, Confocal projection images of the brain counter-labelled with presynaptic antibody nc82 (magenta). *eyFLP* was used to restrict Gal4-mediated *GFP* expression to the eye and antenna. *F-GAL4* labels JO neurons innervating all zones of the AMMC (left), whereas *nompC-GAL4* labels subgroup-B neurons and a subset of subgroup A, but not subgroups CE (right).

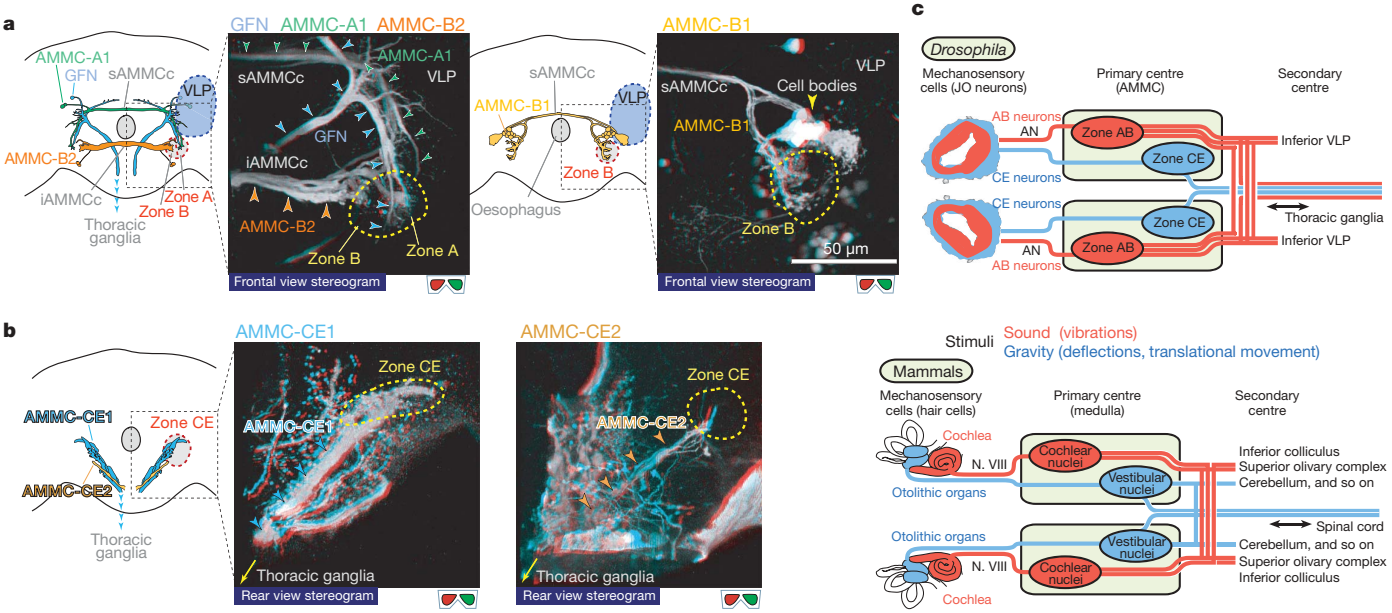


**Figure 6 | Higher-order neurons in the AMMC. a**, Diagrams (left) and three-dimensional confocal projection stereograms (right, for red/green glasses) of higher-order neurons arborizing in the target zones of subgroups AB. AMMC zones and the VLP are highlighted. Arrowheads point to AMMC-A1, -B1 and -B2 neurons and the GFN. The neural pathway downstream of subgroups-AB neurons displays a secondary centre in the inferior VLP and commissural connections between hemispheres. sAMMCc/iAMMCc, superior/inferior AMMC commissures (commissures above and below the oesophagus connecting AMMCs). **b**, Diagram and three-dimensional confocal projection images of higher order neurons arborizing in the target zones of subgroups CE. Arrowheads indicate the structure of AMMC-CE1 and -CE2 neurons, respectively. Subgroups CE neurons have direct connections with the descending tracts to the thoracic ganglia. **c**, Schematic comparison of mechanosensory pathways in flies and mammals. AN, antennal nerve; N. VIII, eighth cranial nerve. For details, see Supplementary Information footnote 8.

between these zones and the VLP were identified either. These zones, however, were abundantly contributed to by descending and ascending neurons to and from the thoracic ganglia (Fig. 6b and Supplementary Fig. 6a). Together, the tight commissural connection in the pathways downstream of sound-sensitive JO neurons and abundant descending tracts downstream of gravity-sensitive JO neurons are reminiscent of the connectivities of mammalian auditory and vestibular pathways (Fig. 6c), the former of which has extensive binaural interactions between the secondary centres of both hemispheres[6,38] whereas the latter has direct descending pathways from the primary centre to the spinal cord[7,39,40] (for more detail, see Supplementary Information footnote 8).

## Discussion

Housing almost 480 primary mechanosensory neurons[13], JO is the largest mechanosensory organ of the fruitfly. We have shown that this organ serves at least two mechanosensory submodalities that are segregated at the level of the primary neurons. JO neurons of subgroups AB respond preferentially to antennal vibrations; they differ in their frequency characteristics, express the NompC channel, and have a role in sound detection. JO neurons of subgroups CE respond preferentially to static deflections, provide information about the forcing direction, do not express the NompC channel, and are required for gravity sensing. As judged from our imaging data and antennal nerve recordings, JO neurons of subgroups CE respond to tiny displacements imposed by the Earth's gravitational field (see Supplementary Information footnote 1 and Supplementary Fig. 3a). Subgroups-CE neurons also respond to large antennal displacements as may be imposed by air jets or wind (see accompanying manuscript[41], Supplementary Information footnote 9 and Supplementary Fig. 3c), indicating either that the same subgroups-CE neurons mediate gravity and wind detection or, alternatively, that sensitive, gravity-responsive CE neurons and less-sensitive, wind-responsive CE neurons may coexist.

As all JO neurons attach to the same antennal receiver, how do their distinct response characteristics come about? The opposing calcium signals evoked by receiver deflections are likely to reflect the opposing connections of JO neurons with the antennal receiver[12,13,19], indicating that these neurons are hyperpolarized by compression and depolarized by stretch (see Supplementary Information footnote 3). The vibration- and deflection-sensitivities of distinct JO neuron subgroups may reflect differences in the molecular machineries for transduction; JO neurons reportedly harbour adapting channels that transduce dynamic receiver vibrations but fully adapt within milliseconds during static receiver deflection[17,19]. Because deflecting the receiver statically for several seconds evokes sustained large-amplitude calcium signals in subgroups CE (Fig. 2a, d), however, also less- or non-adapting channels seem to exist. Transduction channels with different adaptation characteristics seem to occur in many mechanosensory systems, including the mammalian cochlea[42] and also *Drosophila* bristle neurons, which reportedly display mechanically evoked adapting, NompC-dependent and also non-adapting, NompC-independent currents[32]. In the fly's JO, such functional and molecular specializations of the transduction machineries could explain why some neurons preferentially respond to gravity whereas others preferentially respond to sound. The segregation of gravitational and auditory stimuli in the *Drosophila* JO may thus take place at the very first stage of neuronal signal processing.

## METHODS SUMMARY

See Supplementary Information footnote 10 for fly genotypes.

**Stimulation.** The antennal receiver was actuated by feeding voltage commands to an external electrode that served as an electrostatic probe[17]. To allow for attractive and repulsive forcing, the potential of the fly's body was lowered to −15 V against ground[17]. Voltage-force characteristics were flat for frequencies <5 kHz. Acoustic stimuli were used for behavioural and CAP assays. For the equivalence of acoustically and electrostatically induced receiver movements, see ref. 17.

**Calcium imaging.** Fluorescence signals were monitored using a CCD camera (CoolSnap HQ, Roper Scientific) mounted on a microscope (Axioscop2, Carl Zeiss)[22] (also A.K., T.E., M.C.G. and A.F., manuscript in preparation). Each experiment was performed in ≥5 flies. Responses to five repetitive stimuli were averaged. Data acquisition and evaluation were performed as described[22].

**Receiver displacements.** Displacements were measured at the tip of the arista using a Polytec PSV-400 laser Doppler vibrometer[17,18]. In fly strains used for

imaging, receiver fluctuations support the integrity of the antenna and JO neurons[18] (Supplementary Table 1).

**Behavioural assays.** Sound and gravity responses were assayed as described[3,4] (also H.K.I., A.K. and K.I., manuscript in preparation). Between 30 and 50 flies were used for each experiment. Sound detection was examined in six males at a time. To produce intensity profiles (Fig. 4b), males forming courtship chains were scored each 3 s and summed up for 30 s (maximum chain index of 60). For comparisons between flies under silent and sound-stimulated conditions (Fig. 4c, d), scores were summed for 150 s (maximum chain index of 300). For statistical analyses, see Supplementary Information footnotes 4 and 5.

**Nerve recordings.** CAP responses were recorded by means of a tungsten electrode inserted between the antenna and the head. The indifferent electrode was inserted into the thorax. For each genotype, $\geq$7 flies were examined.

**Neuroanatomy.** Serial optical sections of adult fly brains and antennae were captured using confocal microscopes and three-dimensionally reconstructed as described[13]. See Supplementary Methods for detailed equipments.

**Full Methods** and any associated references are available in the online version of the paper at www.nature.com/nature.

**Received 27 June 2008; accepted 20 January 2009.**


1. Toma, D. P., White, K. P., Hirsch, J. & Greenspan, R. J. Identification of genes involved in *Drosophila melanogaster* geotaxis, a complex behavioral trait. *Nature Genet.* **31,** 349–353 (2002).
2. Beckingham, K. M., Texada, M. J., Baker, D. A., Munjaal, R. & Armstrong, J. D. Genetics of graviperception in animals. *Adv. Genet.* **55,** 105–145 (2005).
3. Tempel, B. L., Livingstone, M. S. & Quinn, W. G. Mutations in the dopa decarboxylase gene affect learning in *Drosophila. Proc. Natl Acad. Sci. USA* **81,** 3577–3581 (1984).
4. Eberl, D. F., Duyk, G. M. & Perrimon, N. A genetic screen for mutations that disrupt an auditory response in *Drosophila melanogaster. Proc. Natl Acad. Sci. USA* **94,** 14837–14842 (1997).
5. Tauber, E. & Eberl, D. F. Acoustic communication in *Drosophila. Behav. Processes* **64,** 197–210 (2003).
6. Hudspeth, A. J. in *Principles of Neural Science* (eds Kandel, E. R., Schwartz, J. H. & Thomas, M. J.) 590–613 (McGraw-Hill, 2000).
7. Goldberg, M. E. & Hudspeth, A. J. in *Principles of Neural Science* (eds Kandel, E. R., Schwartz, J. H. & Thomas, M. J.) 801–815 (McGraw-Hill, 2000).
8. Todi, S. V., Sharma, Y. & Eberl, D. F. Anatomical and molecular design of the *Drosophila* antenna as a flagellar auditory organ. *Microsc. Res. Tech.* **63,** 388–389 (2004).
9. Kim, J. *et al.* A TRPV family ion channel required for hearing in *Drosophila. Nature* **424,** 81–84 (2003).
10. Caldwell, J. C. & Eberl, D. F. Towards a molecular understanding of *Drosophila* hearing. *J. Neurobiol.* **53,** 172–189 (2002).
11. Kernan, M. J. Mechanotransduction and auditory transduction in *Drosophila. Pflugers Arch.* **454,** 703–720 (2007).
12. Göpfert, M. C. & Robert, D. The mechanical basis of *Drosophila* audition. *J. Exp. Biol.* **205,** 1199–1208 (2002).
13. Kamikouchi, A., Shimada, T. & Ito, K. Comprehensive classification of the auditory sensory projections in the brain of the fruit fly *Drosophila melanogaster. J. Comp. Neurol.* **499,** 317–356 (2006).
14. Göpfert, M. C. & Robert, D. Biomechanics. Turning the key on *Drosophila* audition. *Nature* **411,** 908 (2001).
15. Baker, D. A., Beckingham, K. M. & Armstrong, J. D. Functional dissection of the neural substrates for gravitaxic maze behavior in *Drosophila melanogaster. J. Comp. Neurol.* **501,** 756–764 (2007).
16. Dickson, B. J. Wired for sex: the neurobiology of *Drosophila* mating decisions. *Science* **322,** 904–909 (2008).
17. Albert, J. T., Nadrowski, B. & Göpfert, M. C. Mechanical signatures of transducer gating in the *Drosophila* ear. *Curr. Biol.* **17,** 1000–1006 (2007).
18. Albert, J. T., Nadrowski, B., Kamikouchi, A. & Göpfert, M. C. Mechanical tracing of protein function in the *Drosophila* ear. *Nature Protocols*. doi:10.1038/nprot.2006.364 (2006).
19. Nadrowski, B., Albert, J. T. & Gopfert, M. C. Transducer-based force generation explains active process in *Drosophila* hearing. *Curr. Biol.* **18,** 1365–1372 (2008).
20. Brand, A. H. & Perrimon, N. Targeted gene expression as a means of altering cell fates and generating dominant phenotypes. *Development* **118,** 401–415 (1993).
21. Miyawaki, A., Griesbeck, O., Heim, R. & Tsien, R. Y. Dynamic and quantitative $Ca^{2+}$ measurements using improved cameleons. *Proc. Natl Acad. Sci. USA* **96,** 2135–2140 (1999).
22. Fiala, A. & Spall, T. *In vivo* calcium imaging of brain activity in *Drosophila* by transgenic cameleon expression. *Sci. STKE* **2003,** pl6 (2003).
23. Göpfert, M. C., Albert, J. T., Nadrowski, B. & Kamikouchi, A. Specification of auditory sensitivity by *Drosophila* TRP channels. *Nature Neurosci.* **9,** 999–1000 (2006).
24. Sharma, Y., Cheung, U., Larsen, E. W. & Eberl, D. F. PPTGAL, a convenient Gal4 P-element vector for testing expression of enhancer fragments in *Drosophila. Genesis* **34,** 115–118 (2002).
25. Benzer, S. Behavioral mutants of *Drosophila* isolated by countercurrent distribution. *Proc. Natl Acad. Sci. USA* **58,** 1112–1119 (1967).
26. Horn, E. & Lang, H.-G. Positional head reflexes and the role of the prosternal organ in the walking fly, *Calliphora erythrocephala. J. Comp. Physiol. [A]* **126,** 137–146 (1978).
27. Sweeney, S. T., Broadie, K., Keane, J., Niemann, H. & O'Kane, C. J. Targeted expression of tetanus toxin light chain in *Drosophila* specifically eliminates synaptic transmission and causes behavioral defects. *Neuron* **14,** 341–351 (1995).
28. McGuire, S. E., Le, P. T., Osborn, A. J., Matsumoto, K. & Davis, R. L. Spatiotemporal rescue of memory dysfunction in *Drosophila. Science* **302,** 1765–1768 (2003).
29. Thum, A. S. *et al.* Differential potencies of effector genes in adult *Drosophila. J. Comp. Neurol.* **498,** 194–203 (2006).
30. Smith, H. K. *et al.* Inducible ternary control of transgene expression and cell ablation in *Drosophila. Dev. Genes Evol.* **206,** 14–24 (1996).
31. Newsome, T. P., Asling, B. & Dickson, B. J. Analysis of *Drosophila* photoreceptor axon guidance in eye-specific mosaics. *Development* **127,** 851–860 (2000).
32. Walker, R. G., Willingham, A. T. & Zuker, C. S. A *Drosophila* mechanosensory transduction channel. *Science* **287,** 2229–2234 (2000).
33. Liu, L. *et al. Drosophila* hygrosensation requires the TRP channels *water witch* and *nanchung. Nature* **450,** 294–298 (2007).
34. Eberl, D. F., Hardy, R. W. & Kernan, M. J. Genetically similar transduction mechanisms for touch and hearing in *Drosophila. J. Neurosci.* **20,** 5981–5988 (2000).
35. Otsuna, H. & Ito, K. Systematic analysis of the visual projection neurons of *Drosophila melanogaster*. I. Lobula-specific pathways. *J. Comp. Neurol.* **497,** 928–958 (2006).
36. Bacon, J. P. & Strausfeld, N. J. The dipteran 'Giant fibre' pathway: neurons and signals. *J. Comp. Physiol. [A]* **158,** 529–548 (1986).
37. Phelan, P. *et al.* Mutations in *shaking-B* prevent electrical synapse formation in the *Drosophila* giant fiber system. *J. Neurosci.* **16,** 1101–1113 (1996).
38. Cant, N. B. & Benson, C. G. Parallel auditory pathways: projection patterns of the different neuronal populations in the dorsal and ventral cochlear nuclei. *Brain Res. Bull.* **60,** 457–474 (2003).
39. Barmack, N. H. Central vestibular system: vestibular nuclei and posterior cerebellum. *Brain Res. Bull.* **60,** 511–541 (2003).
40. Büttner-Ennever, J. A. A review of otolith pathways to brainstem and cerebellum. *Ann. NY Acad. Sci.* **871,** 51–64 (1999).
41. Yorozu, S. *et al.* Distinct sensory representations of wind and near-field sound in the *Drosophila* brain. *Nature* doi:10.1038/nature07843 (this issue).
42. Ricci, A. J., Kennedy, H. J., Crawford, A. C. & Fettiplace, R. The transduction channel filter in auditory hair cells. *J. Neurosci.* **25,** 7831–7839 (2005).


**Supplementary Information** is linked to the online version of the paper at www.nature.com/nature.

**Acknowledgements** We thank D. F. Eberl for JO15, C. J. O'Kane for UFWTRA19, B. J. Dickson for *UAS-GFP S65T* and *eyFLP* fly strains, H. Tanimoto for flies carrying *tubulin-GAL80$^{ts}$* and *UAS-tetanus toxin*, C. Kim for *nan$^{dy5}$*, M. J. Kernan for *nan$^{36a}$*, L. Liu for *nompC-GAL4.25*, A. Wong and G. Struhl for *UAS > CD2, y > CD8::GFP*, J. Urban and G. Technau for MZ-series enhancer trap strains, the members of the NP consortium (a group of eight laboratories in Japan that together produced a large collection of *GAL4* lines) and D. Yamamoto for the NP-series strains, Bloomington Stock Centre for *elav$^{c155}$-GAL4*, D. F. Eberl and C. P. Kyriacou for courtship sound data, S. Fujita for 22C10 antibody, the Developmental Studies Hybridoma Bank for antibodies anti-Elav and nc82, T. Völler for help with calcium imaging, H. Otsuna and K. Shinomiya for preparing some figures, M. Dübbert, K. Öchsner, M. Matsukuma, S. Shuto and K. Yamashita for technical assistance, J. T. Albert, E. D. Hoopfer, B. Nadrowski, K. Endo, H. Otsuna, Y. Hiromi, E. Buchner and N. J. Strausfeld for discussion, and D. J. Anderson and S. Yorozu for sharing unpublished data. This work was supported by the Japanese Cell Science Research Foundation, the Alexander von Humboldt Foundation, and the Japan Society for the Promotion of Science (to A.K.), the DFG Collaborative Research Centre 554 (to A.F.), the Volkswagen Foundation, the BMBF Bernstein Network for Computational Neuroscience, and the DFG Research Centre Molecular Physiology of the Brain (to M.C.G.), and the Human Frontier Science Program Organisation, BIRD/Japan Science and Technology Agency, and the Japan Society for the Promotion of Science (to K.I.).

**Author Contributions** A.K., M.C.G. and K.I. designed research; A.K. and A.F. performed calcium imaging. A.K. and H.K.I. performed fly genetics; H.K.I. performed behavioural and anatomical experiments; T.E. performed nerve recordings; A.K., H.K.I. and O.H. performed histology; A.K., H.K.I., M.C.G. and K.I. wrote the paper; and M.C.G. and K.I. supervised the work. All authors discussed the concepts and results, and commented on the manuscript.

**Author Information** Reprints and permissions information is available at www.nature.com/reprints. Correspondence and requests for materials should be addressed to K.I. (itokei@iam.u-tokyo.ac.jp) or M.C.G. (mgoepfe@gwdg.de).

## METHODS

**Fly stocks.** The following *GAL4* strains were used: JO-all (*F-GAL4*; ref. 9), JO-B (JO2, also known as NP1046; ref. 13), JO-AB (JO15; ref. 24), JO-CE (JO31, also known as NP6250; ref. 13), JO-ACE (JO4, also known as NP6303; ref. 13) and *nompC-GAL4.25* (ref. 33); other strains included *UAS-GFP S65T* (T2 strain) for visualization, *UAS-cam2.1* (*UAS-cameleon2.1-82* (ref. 22) and *UAS-cameleon2.1-76* (ref. 22)) for calcium imaging, *UAS-tetanus toxin* (ref. 27) and *tubulin-GAL80$^{ts}$* (refs 28 and 29) for the selective silencing of neurons, *eyFLP* (ref. 31) and UFWTRA19(ref. 30) for ricin-mediated cell ablation, and *eyFLP* and *UAS > CD2, y > CD8::GFP* (ref. 43) for visualizing neurons from the antenna. To visualize neurons downstream of JO neurons, we screened NP- and MZ-series *GAL4* enhancer trap lines[35]. The Canton-S strain was used as the wild type.

**Calcium imaging.** To enhance reporter signals, flies were made homozygous for both *GAL4* and *UAS-cam2.1*. Only JO-AB was analysed in the heterozygous condition (JO-AB/TM6B) because the antennal mechanics were significantly altered in homozygous JO-AB flies (Supplementary Table 1). After raising flies at 29 °C for 3–15 days to enhance *cam2.1* expression, flies were anaesthetized on ice and affixed onto a coverslip with beeswax. The dorsal tip of the second antennal segment was attached to the coverslip with dental glue, and the gap between the antennae and the coverslip was filled with glycerol. Binning of the cooled CCD camera (CoolSnap HQ, Roper Scientific) was set to give a resolution of 0.645 μm per pixel. A water-immersion ×40 objective (NA = 0.8) was used for imaging. Individual flies were assayed for up to 30 min, with inter-stimulus intervals of 30–60 s. The fluorescence of eCFP and eYFP were captured simultaneously at a rate of 3 Hz with an exposure time of 200 ms. As judged from the mechanical fluctuations of the antennae, the preparation was stable for about 2 h. Only flies with receiver fluctuations indistinguishable from those of the wild-type flies were used for data collection. Receiver displacements used to evoke activities in JO ranged between <5, 10 and 100 μm. Smaller displacements (~1–5 μm) evoked essentially similar response patterns in JO, although with a lower signal-to-noise ratio. Data were analysed off-line with MetaMorph software (Molecular Devices) as described previously[22]. Twenty regions of interest (20 pixels in diameter) were used for analysis, whereby the intensities of eYFP and eCFP fluorescence were normalized to those preceding the stimulus onset ($t = 0$). To compare changes in the eYFP/eCFP ratio across experiments and animals, the mean ratio change at the end of the stimulus was used. Two-tailed Mann–Whitney U-tests were used for statistical analysis because the ratio changes typically did not display a Gaussian distribution. For multiple comparisons, the Sidak–Bonferroni correction was applied[44]. For computing pseudocolour coded ratio changes, the mean of the ratio during the second preceding stimulus onset was subtracted from that during the second preceding the stimulus end.

**Behavioural assay.** Flies were raised on standard medium in a 12 h light/dark cycle at 19 °C to prevent leaky inactivation of *GAL80$^{ts}$* (H.K.I., A.K. and K.I., manuscript in preparation). Flies were collected under ice anaesthesia on the day after eclosion. Wings (song-detection assays) or aristae/antennae (ablation experiments) were removed with fine forceps. The flies were then kept at 19 °C. Negative gravitaxis/phototaxis and sound responses were assayed using 3–7- and 10–14-day-old flies, respectively (when raised at 25 °C, this would correspond to ages of roughly 2–4 and 5–7days). To remove the *GAL80$^{ts}$*-mediated suppression of effecter gene expression, flies were transferred to 30 °C for 24 h before the experiment, and placed back at 19 °C 1 h before the experiment was performed. All assays were carried out at 23–25 °C and 40–60% humidity. Using a countercurrent apparatus[25], we measured startle-induced negative gravitaxis and phototaxis[3]. Gravitaxis was monitored in pitch darkness. Phototaxis was induced by a 40-W fluorescent lamp positioned 30 cm above the centre of the countercurrent apparatus. In brief, we collected flies at the bottom of the tubes by tapping the countercurrent apparatus on the table, and then kept the apparatus still for 30 s to allow the flies to climb the wall. To test the fly's physical ability for climbing the tube wall, phototaxis assay was also performed in a vertical orientation. Five repetitive procedures distributed the flies into six tubes depending on the partition coefficient Cf (that is, their probability of climbing the tubes at each test), which equals mean ± s.e.m. of the weighted mean of the fly numbers in the tubes (see Supplementary Information footnote 4). The Cf value was evaluated as described in Supplementary Information footnote 5. For the sound-response assay, synthesized courtship song[4] was broadcast via a speaker (25 cm in diameter, TAMON S25 W027), with the cone of the speaker being 10 cm away from the centre of the chamber. Behaviour was monitored with a video camera (US522, Panasonic) mounted above the chamber. Recorded movies were converted to serial frames every three seconds, and the number of flies in chains was counted blindly as described[4].

**Evaluation of CAP responses.** CAPs are the summed action potentials that can be recorded extracellularly from the antennal nerve. CAP responses and antennal displacement data were subjected to fast Fourier transforms (FFT) with a resolution of 1 Hz. CAP responses were quantified by measuring their FFT amplitudes at twice the stimulus frequency, because previous observations had shown the frequency doubling of CAP responses[17,34]. Data analysis and statistical data evaluation were performed using Spike 2 (Cambridge Electronic Design), Excel 2004 (Microsoft) and Sigma Plot 10 (Systat Software). Fits were run with a Hill equation consisting of four parameters.

**Immunolabelling of the fly brains and antennae.** Adult brains and antennae were dissected from the progeny of *GAL4* strains and *UAS-GFP S65T* (T2) or *eyFLP*; *UAS > CD2, y > CD8::GFP* crosses and labelled as described previously[13]. The antibodies used were: rabbit anti-GFP polyclonal serum (1:300, Invitrogen) and mouse monoclonal antibodies nc82 (1:20, Developmental Studies Hybridoma Bank), 22C10 (1:50, gift from S. Fujita) and rat polyclonal antibody anti-Elav (1:250, Developmental Studies Hybridoma Bank) for primary antibodies, and Alexa Fluor 488 goat anti-rabbit IgG (1:300, Invitrogen), Alexa Fluor 568 goat anti-mouse IgG (1:300, Invitrogen) and Alexa Flour 633 goat anti-mouse IgG (1:300, Invitrogen) for secondary antibodies. Incubations with primary and secondary antibodies were 72 h and 48 h, respectively.

43. Wong, A. M., Wang, J. W. & Axel, R. Spatial representation of the glomerular map in the *Drosophila* protocerebrum. *Cell* **109**, 229–241 (2002).
44. Keppel, G. & Wickens, T. D. *Design and Analysis: A Researcher's Handbook* 4th edn (Prentice Hall, 2004).